British Journal of Pharmacy

http://doi.org/10.5920/bjpharm.1010

British Journal of Pharmacy

www.bjpharm.hud.ac.uk

Research Article

Effect of Citric Acid concentration on the Physicochemical Properties and Release Profile of Ibuprofen-loaded *Digitaria exilis* Starch Nanoparticles

J. E. John[1,3], B. A. Tytler[1], J. D. Habila[2], Y. E. Apeji[1*], A. Dada[3], C. Y. Isimi[3]

[1]Department of Pharmaceutics and Industrial Pharmacy, Ahmadu Bello University, Zaria, Nigeria.

[2]Department of Chemistry, Ahmadu Bello University, Zaria, Nigeria

[3]Department of Pharmaceutical Technology and Raw Materials Development, NIPRD, Abuja.

ARTICLE INFO

Received: 04/01/2022
Revised: 25/06/2022
Accepted: 28/03/2023
Published: 12/04/2023

*Corresponding author.
Tel.: +234 8063991831
E-mail: yehonathanapeji@gmail.com

KEYWORDS: Citric acid; starch; Digitaria exilis; nanoparticles

ABSTRACT

Nanoparticulate drug delivery systems (NPDDS) have been exploited to overcome the limitations of oral drug delivery. This study evaluated the physicochemical properties of starch citrate and release profile of Ibuprofen from *Digitaria exilis* starch nanoparticles prepared by the nanoprecipitation method in the presence of Tween 80. Nanoparticles were obtained by preparing starch citrate at different concentrations (10 %, 20 % and 30 %) using citric acid, it was dissolved in sodium hydroxide solution (30 % $^{w}/_{w}$) and precipitated with absolute ethanol. Physicochemical characterization of native and cross-linked *Digitaria exilis* starch were undertaken, including FTIR, DSC and XRD. The Encapsulation efficiency, loading capacity, particle size, polydispersity index, SEM, *in-vitro* release and release kinetics of the nanoparticles were also undertaken. Results show that cross-linking significantly influenced the physicochemical properties of native starch. FTIR reveals an introduction of a C=O group at 20 % concentration of CA, which produced particles in the nanometre range (933 nm), with a smooth and spherical structure revealed by SEM. The cross-linked nanoparticles at 20 % showed a controlled release, with the highest cumulative drug release of 40.44 % in 24 h. Citric acid cross-linked *D. exilis* starch can be utilized as a cost-effective vehicle for the sustained delivery of biomolecules.

BY 4.0 Open Access 2023 – University of Huddersfield Press

INTRODUCTION

Nanotechnology has in recent years been utilized in the synthesis of starch nanoparticles, and are characterised by particle size of 1-1000 nm (Zhang *et al.,* 2022). Because of their mechanical properties and renewable nature, different applications of starch-based nanoparticles have been studied (Liu *et al.*, 2017; Simi & Abraham, 2007; Zohreh *et al.*, 2016). Therefore, synthesis and characterization of starch nanoparticles is currently an ongoing research area as the selection of size and shape of the nanoparticles provides effective control over many of the physical and chemical properties of starch (Dar *et al.,* 2013).

Natural polymers are bio-renewable materials obtained from diverse sources that can be degraded into water, carbon dioxide, and inorganic molecules. They are eco-friendly and possess functional groups that can be modified either by physical, chemical, biological, or enzymatic means to yield products with high functionalities. Starch is one of such natural polymers and considered the second most abundant biomass material in nature and found in plant roots, stalks, crop seeds, and staple crops such as rice, corn, wheat, tapioca, and potato

http://doi.org/10.5920/bjpharm.1010

(Corre *et al.*, 2010). They are hydrophilic because of the numerous hydroxyl groups they possess, which makes them susceptible to brittleness, viscosity, retrogradation during storage, poor processibility, changes in crystallinity, texture, colour, etc., hence limiting their use in the development of starch-based products (Qin *et al.*, 2016). Modification of starch involves the alteration of the physical and chemical properties of native starch to improve its functionality. When modified, starch derivatives are by-products of either glucosidic bond cleavage during acid hydrolysis, the introduction of new functional groups (carbonyl) during oxidation, or substitution of starch hydroxyl groups due to etherification or esterification, or cross-linking reactions (Tharanathan, 2005). Some of these enhanced properties include increased tensile strength of starch films (Lu *et al.*, 2019; Kumar *et al.*, 2018) improvement in the mechanical and barrier properties of starch nanoparticles (Silva et al., 2018).

The most extensively utilized technique for the synthesis of nanoparticles from carbohydrate polymers is by chemical means. Cross-linking is a common method employed to reduce starch retrogradation as well as to improve its performance for various applications (Sanchez-Gonzalez *et al.*, 2015). This technique involves the use of multifunctional group reagents (such as hydrophobic ester groups) to react with the hydroxyl groups of starch (responsible for its hydrophilicity), to produce new chemical bonds within molecular starch chains (Ghanbarzadeh *et al.*, 2011; Shi *et al.*, 2007; Zhou *et al.*, 2008). When cross-linked, starch shows improved swelling properties, biodegradability, biocompatibility, high temperature and high shear conditions in addition to the ease of processing, enhanced strength and stability of starch products, thus showing promise as effective carriers for drug delivery (Jyothi *et al.*, 2006; Narendra & Yang, 2009; Wang *et al.*, 2015). Citric acid (CA) is a non-toxic and inexpensive tricarboxylic acid that has found usefulness as a cross-linking agent due to its ability to form covalent linkages with the hydroxyl groups of starch (Wu *et al.*, 2019). Several studies have been conducted on the use of citric acid in starch-based films (Menzel *et al.*, 2013; Narendra & Yang, 2009; Olsson *et al.*, 2013; Seligra *et al.*, 2015), hydrogels (Matheus et al., 2020; Rocha-garcía *et al.*, 2017) and starch nanocomposites (Jose & Al-Harthi, 2017); (J. Zhou et al., 2016). Citric acid has also been used to cross-link other starches, like cyperus starch (Olayemi *et al.*, 2021); potato starch (Wu *et al.*, 2019); rice starch (Butt *et al.*, 2019) and *Digitaria exilis* starch (Isah *et al.*, 2017). However, there are limited studies to show citric acid cross-linked *D exilis* starch nanoparticles.

Fonio (*Digitaria exilis*), commonly known as acha is reported to be one of the earliest cereals found on the African continent. It has been grown for years as a major food source and has been incorporated as a key aspect of nutrition among the people, particularly for its flavour (Jideani, 2000). Compared to other cereals such as maize, millet and sorghum, Fonio has been little used or studied, however, several published reports have appeared in the last decade (Dansi *et al.*, 2006; Ibrahim and Saidu, 2017; Jideani, 2000; Wakil and Olorode, 2018). Studies have shown that *D. exilis* contains impervious starch, and these starches are continuously been investigated for the control of sugar and insulin levels (Pasupuleti and Anderson, 2008). The study conducted by Emeje *et al.*, (2012) also revealed the significance of this starch source. Ibuprofen is a phenylpropionic acid, recognized as a non-prescription over the counter NSAID and belongs to class II of the Biopharmaceutical Classification of drugs, having low solubility at pH 1.2 and 4.5 and high solubility at pH 6.8 but high permeability (Alvarez *et al.*, 2011). It is given at a dose of 600 to 800 mg/d, and up 2400 to 3200 mg/d can be taken for the treatment of painful inflammatory conditions such as rheumatoid arthritis, however, it is associated with side effects (Moore *et al.*, 2015). The aim of this study, therefore, is to evaluate the effects of concentration of citric acid on the physicochemical properties of *D exilis* starch and nanoparticles for the sustained release of Ibuprofen from synthesized nanoparticles.

http://doi.org/10.5920/bjpharm.1010

MATERIALS AND METHODS

Materials

Digitaria exilis (Stapf) grains were purchased from Karmo market, Abuja, and identified in the Medicinal Plant Research Department, NIPRD, Abuja. Tween 80, Ethanol and Sodium Hydroxide (NaOH) were purchased from Finlab, Nigeria Ltd, Citric acid (CA), Ibuprofen powder and Potassium dihydrogen phosphate were purchased from Bristol Scientific Co. Ltd (Nigeria), and the distilled water was obtained from the Department of Pharmaceutical Technology and Raw Materials Development, NIPRD, Abuja

Methods

Starch Extraction

The method of Kunle *et al.*, (2003) was adopted with slight modifications. *Digitaria exilis* (Stapf) grains were weighed and washed with a sufficient amount of water to remove dirt and sand. It was soaked in water containing 0.075 % w/v sodium metabisulphite for 24 h, steeped, and rinsed with water containing sodium metabisulphite. Afterward, it was milled to a fine paste and then transferred to a large bowl containing 10 L of freshly prepared water. The slurry was sieved using a muslin cloth and thereafter, allowed to stand for 12 h. The sediment obtained was further centrifuged at 4500 rpm for 30 min to obtain the starch (this was repeated several times to obtain the plain starch, indicated by the DSC thermograph in Figure 2), which was air-dried for 6 h and thereafter, dried in an oven at 50 ˚C for 16 h. The resulting powder was pulverized, passed through a 250 µm mesh sieve, dried again at 50 ˚C, and packed in an airtight container for further analysis.

Preparation of Cross-linked Starch

The method of Moses *et al.* (2012) was adopted with slight modifications. Citric acid cross-linked starch (30 % w/w) was prepared by dissolving 15 g of CA in 15 mL of distilled water, which was made up to 50 mL in a beaker. *Digitaria exilis* starch (50 g) was added to the resulting solution and mixed thoroughly for 30 mins, after which, it was transferred to a tray and allowed to dry for 48 h at 25 ˚C to effect cross-linking. The resulting cross-linked starch was further dried at 60 ˚C for 6 h in the oven and then pulverized, passed through a 250 µm mesh sieve, and packed in an air-tight container for further analysis. This was performed for different concentrations of CA as shown in Table1.

Table 1. Formulation parameters for cross-linked starch.

Formulation	CA 10	CA 20	CA 30
Weight of starch (g)	50	50	50
Weight of CA (g)	5	10	15
Total Weight (g)	55	60	65

CA = Citric Acid (at 10, 20 and 30 % concentrations)

Preparation of Ibuprofen–Loaded Cross-Linked Starch Nanoparticles

The method of (El-Feky *et al.*, 2015) was adopted with some modifications. Ibuprofen-loaded cross-linked starch nanoparticles was prepared by the nano-precipitation method. The *D. exilis* starch and cross-linked starch (5 $\%^{w}/_{v}$) was dissolved in sodium hydroxide solution (30 $\%\ ^{w}/_{w}$) with the aid of a magnetic stirrer for a period of 1 hr at 25 ˚C. When fully dissolved, 0.5 % of Tween 80 was added while stirring for another 5 min. Afterward, 10 $\%\ ^{w}/_{w}$ of the drug was added and further stirred for 5 min. Absolute ethanol was added drop-wise to the starch solution under high magnetic stirring to produce nano-precipitates. This was centrifuged at 4,500 rpm for 30 min to collect the nanoparticles, lyophilized, and then packed in air-tight jars for further analysis. The composition of nanoparticle formulation is shown in Table 2

Table 2. Composition of Ibuprofen-loaded native and cross-linked starch nanoparticles

Ingredients	NSNP	CA 10	CA 20	CA 30
Ibuprofen (g)	0.5	0.5	0.5	0.5
Quantity of native and modified starch (g)	5	5	5	5
Quantity of NaOH (g)	1.5	1.5	1.5	1.5
Ethanol (mL)	100	100	100	100
Tween 80 (mL)	0.5	0.5	0.5	0.5
Water (mL)	100	100	100	100

NSNP = Native starch nanoparticles; CA = Citric Acid cross-linked starch (at 10, 20 and 30 % concentrations)

http://doi.org/10.5920/bjpharm.1010

Physicochemical Characterisation of *Digitaria exilis* Starch, Cross-Linked Starch and Ibuprofen-Loaded Starch Nanoparticles

Organoleptic Properties of Starch

The organoleptic properties of the extracted starch were carried out by evaluating the taste, colour, odour, appearance, and texture of the starch obtained. This was done by 6 assessors.

Percentage Yield

The percentage yield of extracted starch and starch nanoparticles was calculated as the weight of the starch/starch nanoparticles obtained with respect to the original weight of the starting material. It was calculated using the equation given below:

$$Yield\ (\%) = \frac{Actual\ yield}{Theoretical\ yield} X\ 100\% \ldots\ldots\ldots\ldots\ldots\ldots\ldots\ldots\ldots\ldots\ldots 1$$

pH measurement

The pH of the native and cross-linked starch was measured using a pH meter (Mettler Toledo, Switzerland) with a microprocessor. A 1 % solution of the native and cross-linked starch was prepared and the pH was taken at room temperature (25 ± 2 ˚C). This was performed in triplicates.

Moisture Content

The moisture content of native and cross-linked starch was determined with the aid of a moisture balance (OHAUS MB 45). One gram of the native and cross-linked starch was weighed on a weighing balance (Mettler Toledo ME 303E, Switzerland) and placed in the moisture content analyser that was set at 100 ˚C for 10 min. Moisture content determination was performed in triplicate and the results were obtained by using equation 2 below.

$$Moisture\ Content\ (\%) = \frac{Initial\ weight - final\ weight}{Initial\ weight} X\ 100 \ldots\ldots\ldots\ldots\ldots\ldots\ldots 2$$

Angle of repose, Bulk and Tapped Densities, Carr's Index and Hausner Quotient

A glass funnel of 1 cm orifice was clamped to a retort stand 10 cm to the surface. Two grams of the native and cross-linked starch was gently poured into the funnel and allowed to flow to form a conical heap. The height and radius (r) of the powder heap were determined. The procedure was performed in triplicate and the angle of repose (θ) computed using equation 3.

$$\theta = \tan - 1\left(\frac{\mathrm{h}}{\mathrm{r}}\right) \ldots\ldots\ldots\ldots\ldots\ldots\ldots\ldots\ldots\ldots 3$$

Bulk and tapped densities were determined using the method outlined in the USP (USP, 2007). The volume occupied by 2 g sample weight was determined and taken as its bulk volume. The tapped volume was determined by tapping to constant volume with a Stampfvolumeter (Sav-2003, Germany). The bulk and tapped volume measurements were done in triplicates. The bulk and tapped densities were calculated using Equation 4 and 5 respectively.

$$Bulk\ density\ \left(\frac{g}{ml}\right) = \frac{Weight\ of\ sample\ (g)}{Bulk\ volume\ (ml)} \ldots\ldots\ldots\ldots\ldots\ldots\ldots\ldots 4$$

$$Tapped\ density\ \left(\frac{g}{ml}\right) = \frac{Weight\ of\ sample\ (g)}{Tapped\ Volume\ (ml)} \ldots\ldots\ldots\ldots\ldots\ldots\ldots\ldots 5$$

Carr's index and Hausner quotient were computed from the bulk and tapped densities using equations 6 and 7 respectively.

$$Carr's\ Index = \frac{Tapped\ Density - Bulk\ Density}{Tapped\ density} X\ 100 \ldots\ldots\ldots\ldots 6$$

$$Hausner\ Quotient = \frac{Tapped\ Density}{Bulk\ Density} \ldots\ldots\ldots\ldots\ldots\ldots\ldots\ldots\ldots\ldots 7$$

Swelling Capacity

The swelling capacity was carried out by making a dispersion of 1 g of native and cross-linked starch in 10 mL of distilled water in pre-weighed centrifuge tubes. This was placed in a water bath (Karl Kolb Sci. Co, Germany) equilibrated at 35, 50, 65, 80, and 90 ˚C and the samples were allowed to agitate for 30 min. The swollen starch gel was cooled to 25 ˚C, centrifuged at 1,500 rpm for 10 min and the supernatant was discarded. The weight of the tubes with the swollen starch gels was further weighed and the swelling capacity calculated using equation 8:

http://doi.org/10.5920/bjpharm.1010

$$Swelling\ Capacity = \frac{weight\ of\ swollen\ granules}{weight\ of\ dry\ sample} \ldots\ldots\ldots\ldots\ldots\ldots\ldots\ldots 8$$

Fourier Transform Infra-Red (FTIR) Analysis

Fourier-transform infrared spectroscopy (Cary 630, Agilent technologies, USA) was performed on the native and cross-linked starch to determine and identify the functional groups present. The analysis was conducted at room temperature within a range of 4000–400 cm^{-1}, at a resolution of 2 cm^{-1} using the potassium bromide (KBr) pellets technique. About 5 mg of finely ground solid sample was mixed with 100 mg of dry potassium bromide, and a 7 mm pellet was formed under high pressure. The background and sample spectra were obtained from 64 scans.

Thermal Analysis using Differential Scanning Calorimetry (DSC)

Thermal analysis of the native and cross-linked starch was carried out using Differential Scanning Calorimeter (DSC: Mettler Toledo, Switzerland). Accurately weighed sample (~3–5 mg) was placed in a sealed aluminium pan with a pierced lid. A heating rate of 5 °C/min from °C to 250 °C was applied under nitrogen purging at 20 mL/min.

X-Ray Diffraction (XRD) Analysis

XRD patterns of the native starch and cross-linked starch at 20 % concentration, were obtained on the X-ray diffractometer (Rigaku Miniflex 600, Japan), by utilizing the reflection-transmission spinner stage using the 2θ settings. Two-Theta starting position was 4-75° with a 2θ step of 0.026261 at 8.67 seconds per step. Tube current was 40mA and the tension was 45VA. A Programmable Divergent Slit was used with a 5mm Width Mask and the Gonio Scan was used.

Encapsulation Efficiency (EE)

The encapsulation efficiency of drug-loaded nanoparticles was determined by utilizing the supernatant obtained when the nanoparticles were prepared. After centrifuging at 4,500 rpm for 30 min, an aliquot of the supernatant was assayed for non-bound drug concentration using the UV spectrophotometer (Cary-60, UV-Vis, Agilent technologies, UK) which was read at 215 nm. The drug encapsulation was calculated using equation 9:

$$EE\ (\%) = \frac{Amount\ of\ drug\ in\ prepared\ NPs\ (mg)}{Theoretical\ amount\ of\ drug\ in\ NPs\ (mg)} X\ 100 \ldots 9$$

Drug Loading Capacity (LC)

The drug loading capacity of each batch of ibuprofen-loaded nanoparticles was determined by evaluating the actual content of the drug in nanoparticles to the weight of the nanoparticles. These values were obtained after EE was evaluated and it was calculated using equation 10.

$$LC\ (\%) = \frac{Weight\ of\ drug\ in\ NPs\ (mg)}{Weight\ of\ NPs\ (mg)} X\ 100 \ldots\ldots\ldots\ldots\ldots\ldots\ldots 10$$

Particle Size Analysis (PSA) and Polydispersity Index (PDI)

The particle size and polydispersity index of drug-loaded nanoparticles were obtained using a Zeta sizer (Zen 1600, UK). A colloidal suspension of the nanoparticles was prepared and poured into the nano-sizer cell and the analysis was performed at 25 °C, with a detection angle of 90°.

Scanning Electron Microscopy (SEM)

The scanning electron microscope (Joel-JSM 7600F, Germany) was used to determine the morphology, shape, and surface characteristics of ibuprofen-loaded nanoparticles. The sample was prepared by sprinkling the dispersed nanoparticles onto double-sided adhesive carbon conductive tape which was mounted on a microscopic stub of copper. Then the sample was sputter-coated with gold using ion sputtering device of the equipment

***In-vitro* Release Studies**

The *in-vitro* drug release study was performed in a phosphate buffer (pH 6.8) solution using a 6-station RC-6 dissolution machine. Compressed tablets containing ibuprofen-loaded nanoparticles were placed in the dissolution basket containing 900 mL of the dissolution media and maintained at 37 °C under mild agitation (50 rpm). At pre-determined time interval, 5 ml of the media was withdrawn and replaced with an equal volume of fresh buffer solution to maintain sink conditions. The samples were analysed using the UV spectrophotometer (Cary-60,

http://doi.org/10.5920/bjpharm.1010

UV-Vis, Agilent technologies, UK) at 215 nm (Ganesh & Lee, 2013).

In-vitro Release Kinetics

To evaluate the release kinetics of ibuprofen from native and cross-linked starch nanoparticles, the data obtained from *in-vitro* dissolution studies were fitted into five (5) kinetic models, which include the zero-order, first-order, Higuchi, Hixson-Crowell and Korsmeyer-Peppas kinetic models. The equations representing these kinetic models are given as follows:

Zero Order Kinetics $Qt = Kot \ldots\ldots\ldots\ldots\ldots\ldots\ldots\ldots 11$

First Order Kinetics $\log Q0 - \log Qt = \left(K1\frac{t}{2.303}\right) \ldots 12$

Higuchi Kinetic Model $Qt = KH\sqrt{t} \ldots\ldots\ldots\ldots\ldots\ldots\ldots 13$

Hixson-Crowell Model $(Q0^{1/3} - Qt^{1/3}) = KHC\,t \ldots\ldots 14$

Korsmeyer–Peppas Model $Qt = K_{KP}\,t^{n} \ldots\ldots 15$

where t is the time, Q_t is the amount of drug released at time t, Q_0 is the initial amount of drug in the nanoparticles, K_0 is the zero-order rate constant, K_1 is the first-order rate constant, K_H is the Higuchi constant showing the design variables, K_{HC} is the Hixson-Crowell rate constant, K_{KP} is the Korsmeyer–Peppas rate constant and n is the release exponent (Chourasiya *et al*., 2016).

RESULTS AND DISCUSSION

Percentage Yield and Organoleptic Properties of *Digitaria exilis* Starch

Digitaria exilis starch was obtained, with a yield of approximately 25 %. The starch had a characteristic white colour, with a smooth texture that was odourless and bland in taste. Alaka and Akinoso (2017), Musa *et al*. 2008, and Jideani and Jideani (2011) had a yield of 60, 58.6, and 43.6 % respectively, these were found to be greater than the yield obtained in this study. The reasons for differences in yield and compositional quality can be attributed to the storage temperature (Tadeu *et al.,* 2014), reduced conversion of sucrose to starch (Zi *et al.,* 2018), extreme temperatures and precipitating conditions during harvest (Powell & Reinhard, 2016), sowing and harvesting dates (Ozturk *et al.,* 2008), soil water storage (Butts *et al.,* 2019), the stage and time of harvest (Rahman *et al.,* 1999), and global climate change (Jin *et al.,* 2018).

Physicochemical Properties of Native and Cross-linked *Digitaria exilis* Starch

The ease of handling, storage, and processing of pharmaceutical powders are greatly dependent on their functional properties (Jallo *et al.,* 2012). The physicochemical and flow properties of native and CA modified *D. exilis* starch are shown in Table 3.

Based on the standard flow properties (USP 35, 2012), it can be observed that all the powders had fair to poor flow. Bulk density is a measure of the weightiness of a powder sample. Cross-linking with CA decreased both bulk and tapped densities of *D. exilis* starch (Suravanichnirachorn *et al.,* 2018). The result in this study was found to be lower compared to that obtained by Ngoma *et al.,* (2019) and Anyasi *et al.,* (2017), but contradicts those obtained by Giyatmi & Lingga, (2019). These parameters were not significantly different among the CA cross-linked starch. Likewise, cross-linking did not significantly affect the flow properties of native *D. exilis* starch. Both native and cross-linked starch had fair to poor flow, with CA cross-linked starch at 20 % concentration having the poorest flow in terms of Hausner ratio, Carr's index, and Angle of repose (1.40, 28.78 % and 45 °) respectively.

Table 3. Physicochemical properties of native and cross-linked Digitaria exilis starch

Material	CA-10	CA-20	CA-30	NS
Bulk Density (g/ml)	0.46 ± 0.01	0.45 ± 0.01	0.47 ± 0.01	0.56 ± 9.03
Tapped Density (g/ml)	0.61 ± 0.01	0.57 ± 0.01	0.59 ± 0.01	0.76 ± 0.02
Hausner's Ratio (%)	1.34 ± 0.03	1.40 ± 0.02	1.27 ± 0.06	1.36 ± 0.08
Carr's Index (%)	25.17 ± 1.74	28.78 ± 0.82	21.03 ± 3.44	26.3 ± 1.97
Angle of Repose (°)	35.80	45.10	39.70	46.30
pH	2.97 ± 0.02	2.79 ± 0.02	2.58 ± 0.02	5.11 ± 0.19
Moisture Content (%)	11.81 ± 0.01	11.35 ± 0.03	11.76 ± 0.01	11.00 ± 0.02

CA = Citric Acid cross-linked starch (at 10, 20 and 30 % concentrations); NS = Native starch

The moisture content and pH of native and cross-linked *D. exilis* starch are presented in table 3. Cross-linking significantly reduced the pH of the native

http://doi.org/10.5920/bjpharm.1010

starch, with a gradual decrease in the pH as the concentration of CA increases. According to Olsson *et al.*, (2013), a decrease in pH is necessary for the formation of ester bonds between the starch molecules and the tri-carboxylic acid, a reaction popularly known as the Fischer-esterification reaction. Qin *et al.*, (2019) also noted that hydrolysis of starch occurs as a consequence of pH, the temperature of the reaction and the concentration of citric acid used, and inter-particulate friction occurs resulting in steric hindrances within the starch granules (Chen *et al.*, 2018). The presence of moisture is said to affect the physicochemical and functional properties of polymers, and lead to an increase in microbial growth (Bharate *et al.*, 2010; Builders & Arhewoh, 2016). The moisture content of NS (11 %) in this study does not vary significantly with that of Musa *et al.* (2008) with a value of 11.6 %, but it was found to be lower than that of Odeniyi *et al.*, (2019) who obtained a value of 14.8 %.

Swelling Capacity of Native and Cross-linked *Digitaria exilis* Starch

The swelling capacities of native and cross-linked starch are depicted in figure 1. Cross-linking reduced the swelling power of the native starch across all the temperatures. This can be due to the development of a gel-like mass within the cross-linked starch which restricts the permeation of water into the starch pastes (Siroha & Sandhu, 2018; Sirivongpaisal, 2018). As the temperature increased, the degree of swelling for both the native and cross-linked starch also increased and peaked at 80 ˚C, as a consequence of loss of granule integrity (Choi & Kerr, 2004) and which also depends on the degree of cross-linking (Desam *et al.*, 2018). Although all the cross-linked starch at the various concentrations showed a reduction in the swelling capacity of native starch, the cross-linked starch at 20 % showed the most reduction in swelling across all temperatures.

Fourier-Transform Infrared (FTIR) Analysis

The IR spectra of *D. exilis* and cross-linked starch are presented in table 4. There are no significant changes observed in the spectra between the native and the cross-linked starch. Although the cross-linked starch retains the characteristics of the native starch, there is an introduction of vibration band at 1871 cm^{-1} on the CA - 20 spectra owing to a C=O vibration as a result of the formation of a citrate bond.

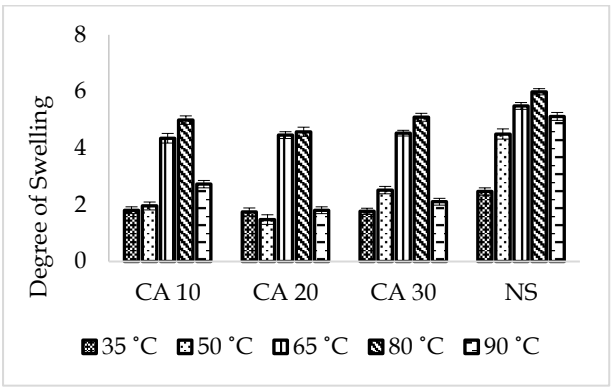

Fig. 1. *Swelling capacity of CA cross-linked and Native D. exilis starch. CA = Citric Acid (at 10, 20 and 30 %); NS = Native Starch.*

Thermal Analysis using Differential Scanning Calorimetry (DSC)

The DSC thermograph of native and cross-linked starch is shown in figure 2. The thermograph of native *D. exilis* starch shows a sharp melting peak with an onset temperature of 59.47 °C, peak temperature of 61.96 °C and an endset temperature of 65.08 °C. Due to the high crystallinity of the native starch, the energy required to melt the granules was shown as the value of ΔH (1032.55 J/g).

Table 4: Fourier Transform Infra-Red absorption bands for native and cross-linked starch

Functional Groups	Infrared Signal Assignment (cm^{-1})			
	NS	CA-10	CA-20	CA-30
O-H Stretch	3257.7	3257.7	3268.9	3265.1
C-H Stretch	2929.7	2926.0	2922.2	2926.0
C=O vibration	-	-	1871.0	-
H_2O absorption band	1640	1651.2	1640.0	1640.0
CH_2-OH side chain	1338.1	1364.2	1364.2	1364.2
C-O vibration	1148.0	1148.0	1148.0	1148.0
C-O-H bend	1077.0	1080.9	1080.9	1080.9
C-O-C vibration	928.1	935.6	931.8	931.8

NS = Native starch; CA = Citric acid cross-linked starch (at 10, 20 and 30 % concentrations

http://doi.org/10.5920/bjpharm.1010

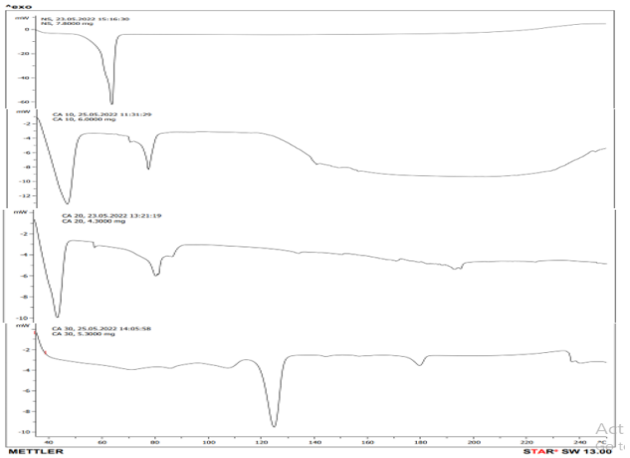

Fig. 2. *Differential scanning thermograph of NS- Native starch, (Topmost) CA = citric acid cross-linked starch (at 10, 20 and 30 %)*

However, cross-linking with citric acid resulted in a shift in the melting peak with onset temperatures of 36.04, 36.76 and 118.40 °C; peak temperatures of 46.30, 43.56 and 124.46 °C; endset temperatures of 50.77, 57.50 and 128.61 °C and Δ*H* values of 710.79, 434.83 and -702.09 J/g for CA-10, 20 and 30 % respectively. The curves for the CA-10 and 20 shifted towards the left, showing a decrease in gelatinization temperature, while CA-30 shifted to the right indicating an increase in the gelatinization temperature. Overall, cross-linking resulted in a notable shift in the gelatinization temperatures. The extent of shift in temperature and the energy required to melt the granules were affected by the concentration of CA used (Dong & Vasanthan, 2020).

X-Ray Diffraction of Native and Cross-linked starch

Native starch commonly exists as A-type spectrum with a granular structure of about 15–45 wt.% crystallinity (Wang *et al.*, 2015; Matzinos *et al.*, 2002). The native *D. exilis* starch (figure 3) shows sharp peaks at 15.2, 17.1, and 18.2° respectively, which shows a typical crystallinity pattern for native starch. However, the citric acid (CA) cross-linked starch at 20 % concentration shows a peak only at 15.1° (figure 3). This result confirms that cross-linking decreased the crystallinity of *D. exilis* starch (Matzinos *et al.*, 2002).

Percentage yield of nanoparticles

The yield of native and CA cross-linked starch nanoparticles as shown in Table 5. Cross-linking reduced the yield of NPs, and a decrease in yield is observed as the concentration of CA increased. When starch is cross-linked with CA, the free hydroxyl groups on starch is replaced by the carboxylic acid groups of CA leading to a reduced tendency of the cross-linked starch to absorb water as a result of inter-granular friction and granule bridging (Hirsch & Kokini, 2002; Su *et al.*, 2019; Woo & Seib, 2002; Woo *et al.*, 2009). Additionally, cross-linking agents causes steric hindrances that produce resistant starches which prevents the swelling of the granules and limit the disintegration of the starch under high shear and pH conditions (Hirsch & Kokini, 2002).

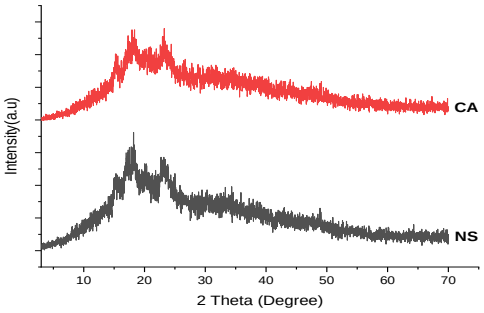

Fig. 3*. XRD pattern of Native and Cross-linked starch at 20 % concentration.*

Table 5. Physicochemical properties of Ibuprofen-loaded cross-linked starch nanoparticles

FORMULATION	CANP 10	CANP 20	CANP 30	NSNP
Yield (%)	62.51 ± 0.01	60.70 ± 0.01	54.12 ± 0.03	66.76 ± 0.02
Encapsulation Efficiency (%)	98.18 ± 0.03	98.24 ± 0.07	98.17 ± 0.04	97.40 ± 0.04
Drug Loading (%)	11.22 ± 0.00	11.56 ± 0.01	12.96 ± 0.00	10.42 ± 0.00
Particle Size (nm)	2019	933	3634	1940
Polydispersity Index	0.912	0.489	1.000	0.531

CANP = Citric acid cross-linked starch nanoparticles (at 10, 20 and 30 % concentrations); NSNP = Native starch nanoparticles

Encapsulation Efficiency (EE)/ Drug Loading Capacity (LC)

Encapsulation efficiency is the total amount of drug that is effectively entrapped within the nanoparticles, expressed in percentage. It also signifies the ability of the drug to be entrapped within the nanoparticle, while drug loading capacity (Loading capacity) is the amount of the active ingredient loaded per weight of the nanoparticle (expressed in percentage). It also signifies the ability of the polymer to entrap the drug. The EE and LC of the native and CA cross-linked

http://doi.org/10.5920/bjpharm.1010

starch NPs are presented in Table 5. Although not significantly different, the EE of the cross-linked starch is higher than the NSNPs. It can also be observed that within the cross-linked starch NPs, CANP at 20 % has a higher EE showing optimum concentration for drug entrapment within the NPs. Cross-linking also increased the LC of NPs as seen in Table 5, with an increase in LC as the concentration of CA increased (El-Naggar *et al.,* 2015). The increase in LC can be attributed to the presence of disulfide linkages within the cross-linked starch NPs (Yang *et al.,* 2014), thereby having more affinity for the drug (Raj & Prabha, 2015) and a greater ability to load more drug than the uncross-linked NPs (Santoyo *et al.,* 2019).

Particle Size/Polydispersity Index

To achieve high efficacy and targeted delivery, the surface properties of NPs are so designed to modulate their cellular uptake and their fate *in vivo* (Steichen *et al.*, 2014; Shen, *et al.*, 2016). Table 5 shows the results of particle size of NPs. The concentration of the CA had a variable effect on the size of the NPs. Only CANP at 20 % concentration had particle size within the nano range (933 nm), suggesting that the concentration of CA to starch ratio at that concentration was the optimum in producing particles below 1000 nm. The size of NSNP closely correlates with the study conducted by Zhou *et al.* (2016) where they obtained starch nanocrystals of mean size 1801 nm. However, when cross-linked with citric acid, they obtained sizes of 503.1, 479.3 and 290.5 nm when heat was applied for 2, 4 and 6 h respectively. Likewise, Ren *et al.* (2018) obtained 1,043.7, 805.6, 1,365.0 nm when they prepared citric acid cross-linked starch nanocrystals and treated with heat for 2, 4 and 6 h respectively compared to control starch nanocrystals (1,834.0 nm). Therefore, particle size of cross-linked starch NPs depend on the treatment method utilized. The polydispersity index (PDI) measures the consistency and the uniform distribution of the dispersed system and has a range between 0 to 1. Values tending towards 0 signifies a uniformly dispersed system, while the reverse is the case with PDI values greater than 0.5.

Scanning Electron Microscopy

Scanning electron microscopy (SEM) is the technique used to obtain surface morphology and composition of a material by utilizing a focused beam of scattered electrons to obtain an image. The SEM image of native and CA cross-linked starch NPs is shown in Figure 4 and 5 respectively.

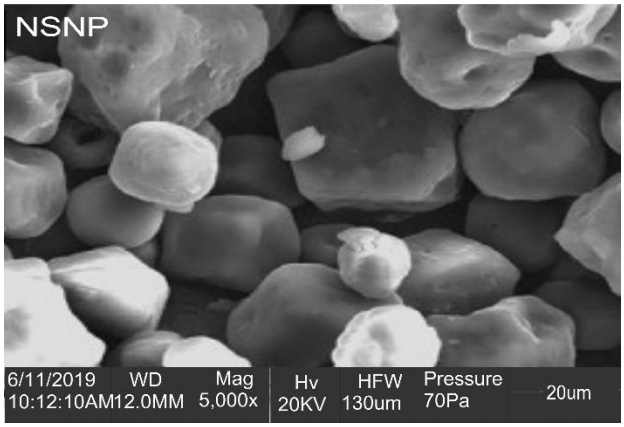

Fig. 4. *Scanning Electron Micrograph of Native starch nanoparticles.*

Cross-linking with CA affects the morphology of native starch, producing smooth and oval-shaped NPs (Chin *et al.,* 2019), while the native starch nanoparticles are polygonal in shape (Shen *et al.*, 2019; Wang *et al.*, 2016). Banerjee *et al.*, (2019) demonstrated that the shape of NPs influences their uptake and passage across intestinal cells and consequently induce a cellular response, that provides useful information on nano-toxicity (Huang *et al.,* 2010). Furthermore, irrespective of other physicochemical properties of NPs, Chu *et al.,* (2014) noted a longer resident time and delayed excretion of sharp-edged NPs when they pierce through cytoplasmic walls.

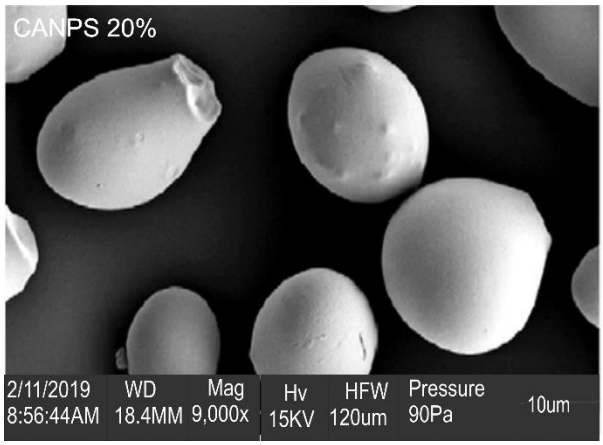

Fig. 5. *Scanning Electron Micrograph of Citric acid cross-linked starch at 20 %.*

http://doi.org/10.5920/bjpharm.1010

In-Vitro Release Studies

The *in vitro* drug release profile of ibuprofen-loaded CA nanoparticles is displayed in Figure 6. The graph shows a distinction between a type of conventional formulation and the nanoparticle formulations. As can be seen, the nano-formulations show the ability of the polymers to hold onto the drug with time suggesting a delayed release of the drug from the polymer, while the pure ibuprofen was released from the formulation within 30 min. The peak plasma concentration of Ibuprofen from an immediate release formulation is usually attained within 60 - 120 min with a bioavailability of 80 - 90 % after oral administration (New Zealand Ltd, 2011). This correlates with the release of the pure drug from the conventional type of formulation. However, for the onset of analgesia, the mean blood plasma concentration of Ibuprofen is between 6.8 - 10.1 µg/mL (Mehlisch and Sykes, 2013). Our study shows a release of ibuprofen from NPs of 21.8 µg/mL (22 %) to 40.8 µg/mL (40.44 %) and 6.5 µg/mL (6.35 %) to 21.7 µg/mL (27.70 %) for CANP and NSNP respectively from 2 to 24 hours. These results therefore show that drug release from the cross-linked starch NPs gave a better result compared to the uncross-linked starch nanoparticles. With the cross-linked NPs, the frequency of dosing can be reduced as this can provide sustained analgesia for over a period of 24 h.

Release Kinetics of Ibuprofen from Optimized Formulations

Table 6 shows the release kinetics of Ibuprofen from CA cross-linked and native starch NPs with plain Ibuprofen as a conventional dosage form. The R^2 values for CANP, NSNP, and plain Ibuprofen are 0.9937, 0.9958, and 0.9831 corresponding to First order, Higuchi, and Korsmeyer–Peppas Models. Accordingly, their release exponent (n) values are 0.0116, 0.0147 and 0.0218. The release pattern of a drug from semi and solid dosage forms is governed by either dissolution or diffusion or both (Barzegar *et al.*, 2008). Drug release refers to the migration of an active ingredient across the concentration gradient from the formulation into the release media and having undergone pharmacokinetic processes becomes available for therapeutic action (Hamidi *et al.*, 2013). Because of this, the key purposes of nano-drug delivery systems from a pharmacokinetic perspective are to enhance *in-vivo* drug release and absorption, increase distribution of the drug at the target site, alter the metabolic drug patterns and extend blood circulation time, while at the same time, delay renal excretion (Hamidi *et al.*, 2013). Therefore, drug release from nano-drug delivery systems influences their therapeutic actions, and studies on the release kinetics will afford essential information into understanding and enhancing such formulations.

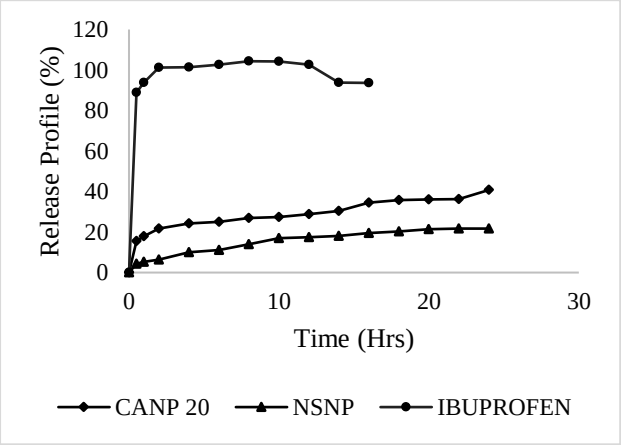

Fig. 6. *In vitro release profile of pure ibuprofen and ibuprofen-loaded native and cross-linked starch nanoparticles.*

Table 6. Data showing the kinetics of release of ibuprofen from native and cross-linked starch nanoparticles

Release Kinetic Models	Zero Order Model		First Order Model		Higuchi Model		Hixson-Crowell Model		Korsmeyer–Peppas Model		
Formulation	K_0	R^2	K_1	R^2	K_H	R^2	K_{HC}	R^2	K_{KP}	R^2	N
CANP 20	24	0.7812	0.5555	0.9937	25.575	0.9378	0.4653	0.9694	1.0246	0.9607	0.0116
NSNP	16.933	0.9128	0.3873	0.9888	17.201	0.9958	0.3774	0.9819	1.5386	0.9717	0.0147
Ibuprofen	103	0.8498	-0.2363	0.7281	107.22	0.9736	0.0454	0.9755	2.9722	0.9831	0.0218

http://doi.org/10.5920/bjpharm.1010

From the results obtained, the CA cross-linked starch NPs followed the first-order kinetic model, signifying that the release of drug is both dissolution and diffusion controlled. While the native starch NPs and plain ibuprofen followed the Higuchi and Korsmeyer–Peppas Models respectively. Factors that affect the release of drug from dosage forms include the physicochemical properties of the solutes, the structural characteristics of the materials used, the release media, and the interactions between these factors on solute diffusion, polymer matrix swelling, and degradation (Fu & Kao, 2011).

CONCLUSION

Nanoparticles were effectively synthesized from *D. exilis* starch via the nanoprecipitation method. The results obtained revealed that concentration of CA had a significant effect on the physicochemical properties of the starch. Further characterization using FTIR shows an introduction of a citrate band in the starch cross-linked with 20 % concentration of citric acid to yield spherical nanoparticles of 933 nm, with improved encapsulation and loading efficiencies, in addition, to a sustained the release of Ibuprofen from the loaded NPs.

REFERENCES

Alaka, A. O., & Akinoso, R. 2017. Physical and chemical properties of sweet juice produced from hydrolysed acha (Digitaria exilis Stapf) starch using crude amylase from germinated maize. *World Scientific News*, *87*, 125–135.

Alvarez, C., Nnez, I., Torrado, J. J., Gordon, J., Potthast, H., & Garc´Ia-Arieta, A. 2011. Investigation on the Possibility of Biowaivers for Ibuprofen. *Journal of Pharmaceutical Sciences*, *100*(6), 1–8. https://doi.org/10.1002/jps.22472

Anyasi, T. A., Jideani, A. I. O., & Mchau, G. R. A. 2017. Effects of organic acid pretreatment on microstructure , functional and thermal properties of unripe banana flour. *Food Measure*, *11*, 99–110. https://doi.org/10.1007/s11694-016-9376-2

Banerjee, A., Qi, J., Gogoi, R., Wong, J., & Mitragotri, S. 2019. Role of Nanoparticle Size, Shape and Surface Chemistry in Oral Drug Delivery. *Science Direct*, *805*, 2–27.

Barzegar-jalali, M., Adibkia, K., Valizadeh, H., Reza, M., & Shadbad, S. 2008. Kinetic analysis of drug release from nanoparticles. *Journal of Pharmacy and Pharmaceutical Sciences*, *11*(1), 167–177.

Bharate, S. S., Bharate, S. B., & Bajaj, A. N. 2010. Interactions and incompatibilities of pharmaceutical excipients with active pharmaceutical ingredients : a comprehensive review. *Journal of Excipients and Food Chemistry*, *1*(3), 3–26.

Butt, N. A., Ali, T. M., & Hasnain, A. 2019. International Journal of Biological Macromolecules Rice starch citrates and lactates: A comparative study on hot water and cold water swelling starches. *International Journal of Biological Macromolecules*, *127*, 107–117. https://doi.org/10.1016/j.ijbiomac.2019.01.019

Butts-wilmsmeyer, C. J., Seebauer, J. R., Singleton, L., & Below, F. E. 2019. Weather During Key Growth Stages Explains Grain Quality and Yield of Maize. *Agronomy*, *9*(16), 1–15. https://doi.org/10.3390/agronomy9010016

Chen, Y., Kaur, L., & Singh, J. 2018. Chemical Modification of Starch. In *Starch in Food* (pp. 283–321). Elsevier Ltd. https://doi.org/10.1016/B978-0-08-100868-3.00007-X

Chin, S. F., Romainor, A. N. B., Pang, S. C., & Lee, B. K. 2019. pH-Responsive Starch-Citrate Nanoparticles for Controlled Release of Paracetamol. *Starch*, 1–9. https://doi.org/10.1002/star.201800336

Choi, S., & Kerr, W. L. 2004. Swelling Characteristics of Native and Chemically Modified Wheat Starches as a Function of Heating. *Starch/Staerke*, *56*, 181–189. https://doi.org/10.1002/star.200300233

Chourasiya, V., Bohrey, S., & Pandey, A. 2016. Formulation, optimization, characterization and in-vitro drug release kinetics of atenolol loaded PLGA nanoparticles using 33 factorial design for oral delivery. *Materials Discovery*, 1–32. https://doi.org/10.1016/j.md.2016.12.002

Chu, Z., Zhang, S., Zhang, B., Zhang, C., Fang, C., Rehor, I., Cigler, P., Chang, H., Lin, G., Liu, R., & Li, Q. 2014. *effects on cellular fate of nanoparticles*. 1–9. https://doi.org/10.1038/srep04495

Corre, D. Le, Bras, J., & Dufresne, A. 2010. Starch Nanoparticles: A Review. *Biomacromolecules*, *11*, 1139–1153.

Dansi, A., Vodouhe, R., & Akpagana, K. 2006. Indigenous knowledge and traditional conservation of fonio millet (Digitaria exilis , Digitaria iburua) in Togo. *Biodiversity and Conservation*, *15*, 2379–2395. https://doi.org/10.1007/s10531-004-2938-3

Dar, M. A., Ingle, A., & Rai, M. 2013. Enhanced antimicrobial activity of silver nanoparticles synthesized by Cryphonectria sp . evaluated singly and in combination with antibiotics. *Nanomedicine: Nanotechnology, Biology, and Medicine*, *9*(1), 105–110. https://doi.org/10.1016/j.nano.2012.04.007

Desam, G. P., Li, J., Chen, G., Campanella, O., & Narsimhan, G. 2018. Prediction of swelling behavior of crosslinked maize starch suspensions. *Carbohydrate Polymers*, *18*, 1–32. https://doi.org/10.1016/j.carbpol.2018.07.020

Dong, H., & Vasanthan, T. 2020. Effect of phosphorylation techniques on structural, thermal, and pasting properties of pulse starches in comparison with corn starch. *Food Hydrocolloids*, 1–29. https://doi.org/10.1016/j.foodhyd.2020.106078

El-Feky, G. S., MH, E.-R., El-Sheikh, M., El-Naggar, M. E., & A, H. 2015. Utilization of Crosslinked Starch Nanoparticles as a Carrier for Indomethacin and Acyclovir Drugs. *Journal of Nanomedicine & Nanotechnology*, *6*(1), 1–9. https://doi.org/10.4172/2157-7439.1000254

El-naggar, M. E., El-rafie, M. H., El-sheikh, M. A., El-feky, G. S., & Hebeish, A. 2015. Synthesis, characterization,

release kinetics and toxicity profile of drug-loaded starch nanoparticles. *International Journal of Biological Macromolecules*, *81*, 718–729. https://doi.org/10.1016/j.ijbiomac.2015.09.005

Emeje, M., Kalita, R., Isimi, C., Buragohain, A., Kunle, O., & Ofoefule, S. 2012. Synthesis, physicochemical characterization, and Functional properties of an esterified starch from an underutilized source in Nigeria. *African Journal of Food, Agriculture, Nutrition and Development*, *12*(7), 27–31. https://doi.org/10.4314/ajfand.v12i7.

Fu, Y., & Kao, W. J. 2011. Drug Release Kinetics and Transport Mechanisms of Non- degradable and Degradable Polymeric Delivery Systems. *Expert Opinion Drug Delivery*, *7*(4), 429–444. https://doi.org/10.1517/17425241003602259.Drug

Ganesh, M., & Lee, S. G. 2013. Synthesis, Characterization and Drug Release Capability of New Cost Effective Mesoporous Silica Nano Particle for Ibuprofen Drug Delivery Synthesis , Characterization and Drug Release Capability of New Cost Effective Mesoporous Silica Nano Particle for I. *International Journal of Control and Automation*, *6*(5), 207–216. https://doi.org/10.14257/ijca.2013.6.5.20

Ghanbarzadeh, B., Almasi, H., & Entezami, A. A. 2011. Improving the barrier and mechanical properties of corn starch-based edible films: Effect of citric acid and carboxymethyl cellulose. *Industrial Crops and Products*, *33*(1), 229–235. https://doi.org/10.1016/j.indcrop.2010.10.016

Giyatmi, & Lingga, D. K. 2019. The effect of citric acid and sodium bicarbonate concentration on the quality of effervescent of red ginger extract The effect of citric acid and sodium bicarbonate concentration on the quality of effervescent of red ginger extract. *Earth and Environmental Science*, *383*, 1–11. https://doi.org/10.1088/1755-1315/383/1/012022

Hamidi, M., Azadi, A., Rafiei, P., & Ashrafi, H. 2013. A Pharmacokinetic Overview of Nanotechnology-Based Drug Delivery Systems : An ADME-Oriented Approach. *Critical Reviews™ in Therapeutic Drug Carrier Systems*, *5*, 435–467.

Hirsch, J. B., & Kokini, J. L. 2002. Understanding the Mechanism of Cross-Linking Agents (POCl 3, STMP, and EPI) Through Swelling Behavior and Pasting Properties of Cross-Linked Waxy Maize Starches 1. *Cereal Chemistry*, *79*(1), 102–107.

Huang, X., Teng, X., Chen, D., Tang, F., & He, J. 2010. The effect of the shape of mesoporous silica nanoparticles on cellular uptake and cell function. *Biomaterials*, *31*(3), 438–448. https://doi.org/10.1016/j.biomaterials.2009.09.060

Ibrahim, H. M., & Saidu, B. 2017. Effect of Processed Acha (Digitaria exilis) grain on glycemic index of diabetes induced Wistar Rat model. *Scholarly Journal of Biological Science*, *6*(3), 89–93.

Isah, S., Oshodi, A. A., & Atasie, V. N. 2017. Physicochemical properties of cross linked acha (digitaria exilis) starch with citric acid. *Chemistry International*, *3*(2), 150–157.

Jallo, L. J., Ghoroi, C., Gurumurthy, L., Patel, U., & Davé, R. N. 2012. Improvement of flow and bulk density of pharmaceutical powders using surface modification. *International Journal of Pharmaceutics*, *423*, 213–225. https://doi.org/10.1016/j.ijpharm.2011.12.012

Jideani, I. A. 2000. Traditional and possible technological uses of Digitaria exilis (acha) and Digitaria iburua (iburu): A review. *Plant Foods for Human Nutrition*, *54*, 363–374.

Jideani, I. A., & Jideani, V. A. 2011. Developments on the cereal grains Digitaria exilis (acha) and Digitaria iburua (iburu). *Journal of Food Science and Technology*, *48*(3), 251–259. https://doi.org/10.1007/s13197-010-0208-9

Jin Wang, Vanga, S. K., Saxena, R., Orsat, V., & Raghavan, V. 2018. Effect of Climate Change on the Yield of Cereal Crops : A Review. *Climate*, *6*(41), 1–19. https://doi.org/10.3390/cli6020041

Jose, J., & Al-Harthi, M. A. 2017. Citric acid crosslinking of poly (vinyl alcohol)/starch/graphene nanocomposites for superior properties. *Iranian Polymer Journal*, 1–9. https://doi.org/10.1007/s13726-017-0542-0

Jyothi, A. N., Moorthy, S. N., & Rajasekharan, K. N. 2006. Effect of cross-linking with epichlorohydrin on the properties of cassava (Manihot esculenta Crantz) starch. *Starch/Staerke*, *58*(6), 292–299. https://doi.org/10.1002/star.200500468

Kumar, S. V., George, J., & Sajeevkumar, V. A. 2018. PVA Based Ternary Nanocomposites with Enhanced Properties Prepared by Using a Combination of Rice Starch Nanocrystals and Silver Nanoparticles. *Journal of Polymers and the Environment*, *26*, 3117–3127. https://doi.org/10.1007/s10924-018-1200-0

Kunle, O. O., Ibrahim, Y. E., Emeje, M. O., Shaba, S., Kunle, Y., Development, M., Insti-, N., Mi-, P., & Bello, A. 2003. Extraction , Physicochemical and Compaction Properties of Tacca Starch – a Potential Pharmaceutical Excipient Research Paper. *Starch - Stärke*, *55*, 319–325.

Liu, G., Gu, Z., Hong, Y., Cheng, L., & Li, C. 2017. Structure, functionality and applications of debranched starch: A review. *Trends in Food Science & Technology*, 1–45. https://doi.org/10.1016/j.tifs.2017.03.004

Lu, H., Ji, N., Li, M., Wang, Y., Xiong, L., Zhou, L., Qiu, L., Bian, X., Sun, C., & Sun, Q. 2019. Preparation of Borax Cross-Linked Starch Nanoparticles for Improvement of Mechanical Properties of Maize Starch Films. *Journal of Agricultural and Food Chemistry*, *67*, 2916–2925. https://doi.org/10.1021/acs.jafc.8b06479

Matheus, B., Cagnin, C., Yamashita, F., Bonametti, J., Salomão, P., Oliveira, D., Victória, M., & Grossmann, E. 2020. Citric acid as crosslinking agent in starch/xanthan gum hydrogels produced by extrusion and thermopressing. *LWT - Food Science and Technology*, *125*, 1–7. https://doi.org/10.1016/j.lwt.2019.108950

Matzinos, P., Tserki, V., Kontoyiannis, A., & Panayiotou, C. 2002. Processing and characterization of starch/polycaprolactone products. *Polymer Degradation and Stability*, *77*, 17–24.

Mehlisch, D. R., & Sykes, J. 2013. Ibuprofen blood plasma levels and onset of analgesia. *International Journal of Clinical Practice*, *67*, 3–8. https://doi.org/10.1111/ijcp.12053

Menzel, C., Olsson, E., Plivelic, T. S., Andersson, R., Johansson, C., Kuktaite, R., Järnström, L., & Koch, K. 2013. Molecular structure of citric acid cross-linked starch films. *Carbohydrate Polymers*, *96*(1), 270–276. https://doi.org/10.1016/j.carbpol.2013.03.044

Moore, N., Pollack, C., & Butkerait, P. 2015. Adverse drug

reactions and drug – drug interactions with over-the-counter NSAIDs. *Therapeutics and Clinical Risk Management*, *11*, 1061–1075.
Musa, H., Muazu, J., Bhatia, P. G., & Mshelbwala, K. 2008. Investigation into the Use of Fonio (Digitaria Exilis) Starch as a Tablet Disintegrant. *Nigerian Journal of Pharmaceutical Sciences*, *7*(1), 67–78.
Narendra, R., & Yang, Y. 2009. Citric acid cross-linking of starch films. *Food Chemistry*, *118*, 1–11. https://doi.org/10.1016/j.foodchem.2009.05.050
New Zealand Ltd, M. 2011. *Ibuprofen Fact Sheet* (pp. 1–12).
Ngoma, K., Mashau, M. E., & Silungwe, H. 2019. Physicochemical and Functional Properties of Chemically Pretreated Ndou Sweet Potato Flour. *International Journal of Food Science*, *2019*, 1–10.
Ntui, V. O., Uyoh, E. A., Nakamura, I., & Mii, M. 2017s. Agrobacterium -mediated genetic transformation of Fonio (Digitaria exilis (L.) Stapf). *African Journal of Biotechnology*, *16*(23), 1302–1307. https://doi.org/10.5897/AJB2017.15903
Odeniyi, M. A., Adepoju, A. O., & Jaiyeoba, K. T. 2019. Native and Modified Digitaria exilis Starch Nanoparticles as a Carrier System for the Controlled Release of Naproxen. *Starch - Stärke*, *71*, 1–10. https://doi.org/10.1002/star.201900067
Olayemi, B., Isimi, C. Y., Ekere, K., Isaac, A. J., Okoh, J. E., & Emeje, M. 2021. Green Preparation of Citric Acid Crosslinked Starch for Improvement of Physicochemical Properties of Cyperus Starch. *Turkish Journal of Pharmaceutical Sciences*, *18*(1), 34–43. https://doi.org/10.4274/tjps.galenos.2019.65624
Olsson, E., Menzel, C., Johansson, C., Andersson, R., Koch, K., & Järnström, L. 2013. The effect of pH on hydrolysis, cross-linking and barrier properties of starch barriers containing citric acid. *Carbohydrate Polymers*, 1–31. https://doi.org/10.1016/j.carbpol.2013.07.040
Olsson, E., Menzel, C., Johansson, C., Andersson, R., Koch, K., & Lars Järnström. 2013. The effect of pH on hydrolysis, cross-linking and barrier properties of starch barriers containing citric acid. *Carbohydrate Polymers*, 1–31. https://doi.org/10.1016/j.carbpol.2013.07.040
Ozturk, O., Topal, A., Akinerdem, F., & Akgun, N. 2008. Effects of sowing and harvesting dates on yield and some quality characteristics of crops in sugar beet/cereal rotation system. *Journal of the Science of Food and Agriculture*, *88*, 141–150. https://doi.org/10.1002/jsfa.3061
Pasupuleti, V. K., & Anderson, J. W. 2008. *Health and Type 2 Diabetes*.
Powell, J. P., & Reinhard, S. 2016. Measuring the Effects of Extreme Weather Events on Yields. *Weather and Climate Extremes*, 1–26. https://doi.org/10.1016/j.wace.2016.02.003
Qin, Y., WentaoWang, Zhang, H., Dai, Y., Hou, H., & Dong, H. 2019. Effects of Citric Acid on Structures and Properties of Thermoplastic Hydroxypropyl Amylomaize Starch Films. *Materials*, *12*, 1–13.
Rahman, M. A., Nahar, N., Mian, A. J., & Mosihuzzaman, M. 1999. Variation of carbohydrate composition of two forms of fruit from jack tree (Artocarpus heterophyllus L.) with maturity and climatic conditions. *Food Chemistry*, *65*, 91–97.
Raj, V., & Prabha, G. 2015. Synthesis, characterization and in vitro drug release of cisplatin loaded Cassava starch acetate – PEG/gelatin nanocomposites. *Journal of Association of Arab Universities for Basic and Applied Sciences*, 1–7. https://doi.org/10.1016/j.jaubas.2015.08.001
Ren, L., YuchenZhang, QianWang, Zhou, J., Tong, J., Chen, D., & Su, X. 2018. Convenient Method for Enhancing Hydrophobicity and Dispersibility of Starch Nanocrystals by Crosslinking Modification with Citric Acid. *International Journal of Food Engineering*, 1–13. https://doi.org/10.1515/ijfe-2017-0238
Rocha-garcía, D., Guerra-contreras, A., Reyes-hernández, J., & Palestino, G. 2017. Thermal and kinetic evaluation of biodegradable thermo-sensitive gelatin/poly (ethylene glycol) diamine crosslinked citric acid hydrogels for controlled release of tramadol. *European Polymer Journal*, 1–47. https://doi.org/10.1016/j.eurpolymj.2017.02.007
Sanchez-Gonzalez, L., Arab-Tehrany, E., Chafer, M., Gonzalez-Martınez, C., & Chiralt, A. 2015. Active Edible and Biodegradable Starch Films ´. *Polysaccharides*, 717–734. https://doi.org/10.1007/978-3-319-16298-0
Santoyo-Aleman, D., Sanchez, L. T., & Villa, C. C. 2019. Citric-Acid Modified Banana Starch Nanoparticles as a Novel Vehicle for β-Carotene Delivery. *Journal of Science and Food Agriculture*, *99*, 6392–6399. https://doi.org/10.1002/jsfa.9918
Seligra, P. G., Jaramillo, C. M., Fama, L., & Goyanes, S. 2015. Biodegradable and non-retrogradable eco-films based on starch-glycerol with citric acid as crosslinking agent. *Carbohydrate Polymers*, 1–16. https://doi.org/10.1016/j.carbpol.2015.11.041
Shen, Y., Zhang, N., Xu, Y., Huang, J., Yuan, M., Wu, D., & Shu, X. 2019. Physicochemical properties of hydroxypropylated and cross- linked rice starches differential in amylose content. *International Journal of Biological Macromolecules*, #pagerange#. https://doi.org/10.1016/j.ijbiomac.2019.01.194
Shen, Z., Nieh, M.-P., & Li, Y. 2016. Decorating Nanoparticle Surface for Targeted Drug Delivery: Opportunities and Challenges. *Polymers*, *8*(3), 83. https://doi.org/10.3390/polym8030083
Shi, R., Zhang, Z., Liu, Q., Han, Y., Zhang, L., Chen, D., & Tian, W. 2007. Characterization of citric acid/glycerol co-plasticized thermoplastic starch prepared by melt blending. *Carbohydrate Polymers*, *69*, 748–755. https://doi.org/10.1016/j.carbpol.2007.02.010
Silva, D., Freitas, F., Lopes, R., Fialho, L., Fialho, L., Christine, E., Cabral, D. M., Ignacio, J., & Velasco, I. 2018. Production and Characterization of Starch Nanoparticles Normane Matta Fakhouri. In *IntechOpen* (pp. 41–48). https://doi.org/10.5772/intechopen.74362
Simi, C. K., & Abraham, E. 2007. Hydrophobic grafted and cross-linked starch nanoparticles for drug delivery. *Bioprocess Biosyst Eng*, *30*, 173–180. https://doi.org/10.1007/s00449-007-0112-5
Sirivongpaisal, P. 2018. Functional properties of dual-modified rice starch. *Journal of Food Science and Agricultural Technology*, *4*, 93–98.
Siroha, A. K., & Sandhu, K. S. 2018. Physicochemical, rheological, morphological, and in vitro digestibility properties of cross-linked starch from pearl millet cultivars. *International Journal of Food Properties*, *21*(1), 1371–1385.

https://doi.org/10.1080/10942912.2018.1489841
Steichen, D. S., Mary, C.-M., & Peppas, N. A. 2014. A review of current nanoparticle and targeting moieties for the delivery of cancer therapeutics. *European Journal of Pharmaceutical Sciences*, *48*(3), 416–427. https://doi.org/10.1016/j.ejps.2012.12.006.A
Su, P., Nikfarjam, N., Deng, Y., & Taheri-qazvini, N. 2019. Pickering emulsion stabilized by amphiphilic pH-sensitive starch nanoparticles as therapeutic containers. *Colloids and Surfaces B: Biointerfaces*, *181*, 244–251. https://doi.org/10.1016/j.colsurfb.2019.05.046
Suravanichnirachorn, W., Haruthaithanasan, V., Suwonsichon, S., Sukatta, U., Maneeboon, T., & Chantrapornchai, W. 2018. Effect of carrier type and concentration on the properties, anthocyanins and antioxidant activity of freeze-dried mao [Antidesma bunius (L.) Spreng] powders. *Agriculture and Natural Resources*, *52*(5), 1–20. https://doi.org/10.1016/j.anres.2018.09.011
Tadeu, R., Levien, N., Moomand, K., Oliveira, M. De, Zavareze, R., Marques, R., Dietrich, C., & Cardoso, M. 2014. Characteristics of starch isolated from maize as a function of grain storage temperature. *Carbohydrate Polymers*, *102*, 88–94.
Tharanathan, R. N. 2005. Starch - Value addition by modification. *Critical Reviews in Food Science and Nutrition*, *45*(5), 371–384. https://doi.org/10.1080/10408390590967702
Wakil, S. M., & Olorode, E. M. 2018. Potential Probiotic Properties of Lactic Acid Bacteria Isolated from Malted and Spontaneously Fermented Acha (Digitaria exilis) Flour. *Advances in Research*, *17*(6), 1–12. https://doi.org/10.9734/AIR/2018/45414
Wang, Hang, Chen, X., Yan, S., Wang, H., Hu, Z., Wang, X., & Huo, M. 2015. Aerobic oxidation of starch catalyzed by isopolyoxovanadate Na4Co (H2O) Aerobic oxidation of starch catalyzed by isopolyoxovanadate. *Carbohydrate Polymers*, *117*, 673–680. https://doi.org/10.1016/j.carbpol.2014.10.066
Wang, Hualin, Lv, J., Jiang, S., Niu, B., Pang, M., & Jiang, S. 2016. Preparation and characterization of porous corn starch and its adsorption toward grape seed proanthocyanidins. *Starch - Stärke*, 1–10. https://doi.org/10.1002/star.201600009
Woo, K. S., Maningat, C. C., & Seib, P. A. 2009. Increasing Dietary Fiber in Foods : The Case for Phosphorylated Cross-Linked Resistant Starch , a Highly Concentrated Form of Dietary Fiber. *Cereal Foods World*, *54*(5), 217–223.
Woo, K. S., & Seib, P. A. 2002. Cross-Linked Resistant Starch: Preparation and Properties. *Cereal Chemistry*, *79*(6), 819–825.
Wu, H., Lei, Y., Lu, J., Zhu, R., Xiao, D., Jiao, C., Xia, R., Zhang, Z., Shen, G., Liu, Y., Li, S., & Li, M. 2019. Effect of citric acid induced crosslinking on the structure and properties of potato starch/chitosan composite films. *Food Hydrocolloids*, *97*, 1–10. https://doi.org/10.1016/j.foodhyd.2019.105208
Yang, J., Huang, Y., Gao, C., Liu, M., & Zhang, X. 2014. Fabrication and evaluation of the novel reduction-sensitive starch nanoparticles for controlled drug release. *Colloids and Surfaces B: Biointerfaces*, *115*, 368–376.
Zhang, Q., Gonelle-gispert, C., Li, Y., & Geng, Z. 2022. Islet Encapsulation: New Developments for the Treatment of Type 1 Diabetes. *Frontiers in Immunogogy*, *13*(April), 1–16. https://doi.org/10.3389/fimmu.2022.869984
Zhou, J., Tong, J., Su, X., & Ren, L. 2016. Hydrophobic starch nanocrystals preparations through crosslinking modification using citric acid. *International Journal of Biological Macromolecules*, 1–37. https://doi.org/10.1016/j.ijbiomac.2016.06.082
Zhou, Y., Wang, D., Zhang, L., Du, X., & Zhou, X. 2008. Effect of polysaccharides on gelatinization and retrogradation of wheat starch. *Food Hydrocolloids*, *22*, 505–512. https://doi.org/10.1016/j.foodhyd.2007.01.010
Zi, Y., Ding, J., Song, J., Humphreys, G., Peng, Y., & Li, C. 2018. *Grain Yield , Starch Content and Activities of Key Enzymes of Waxy and Non-waxy Wheat (Triticum aestivum L.)* (Issue 2). https://doi.org/10.1038/s41598-018-22587-0
Zohreh, H., Hadian, Z., & Mashayekh, M. 2016. Nanocomposites in food packaging applications and their risk assessment for health. *Electronic Physician*, *8*(6), 2531–2538.